Research Square

Preprints are preliminary reports that have not undergone peer review.
They should not be considered conclusive, used to inform clinical practice,
or referenced by the media as validated information.

Plankton diversity, heterogeneous cross-trophic associations and community assembly across four hydrochemically contrasting plateau lakes in northern China

Yi Zhang
Inner Mongolia Environmental Monitoring Center
Wenjie Liu
Dalian Ocean University
Jinrui Zhang
Northeast Tiger and Leopard Biodiversity National Observation and Research Station, Beijing Normal University
Zhendong Wu
Dalian Ocean University
Pan Hu
Dalian Ocean University
Yongli Tian
Inner Mongolia Environmental Monitoring Center
Xinliang Zhao
Inner Mongolia Environmental Monitoring Center
Hao Li
Inner Mongolia Environmental Monitoring Center
Juanjuan Qi
Ulanqab Branch of the Inner Mongolia Environmental Monitoring Center
Rui Wang
Chifeng Branch of the Inner Mongolia Environmental Monitoring Center
Xuwang Yin
yinxuwang@dlou.edu.cn

Dalian Ocean University

Research Article

Keywords: phytoplankton, zooplankton, lake hydrochemistry, salinity, community assembly, Inner Mongolia Plateau

Posted Date: November 13th, 2026

DOI: https://doi.org/10.21203/rs.3.rs-11594130/v1

License: This work is licensed under a Creative Commons Attribution 4.0 International License. Read Full License

Additional Declarations: No competing interests reported.

Plankton diversity, heterogeneous cross-trophic associations and community assembly across four hydrochemically contrasting plateau lakes in northern China

Yi Zhang[1#], Wenjie Liu[2#], Jinrui Zhang[3#], Zhendong Wu[2], Pan Hu[2], Yongli Tian[1], Xinliang Zhao[1], Hao Li[1], Juanjuan Qi[4], Rui Wang[5], Xuwang Yin[2*]

[1]. Inner Mongolia Environmental Monitoring Center, Hohhot, China.

[2]. Liaoning Provincial Key Laboratory for Hydrobiology, College of Fisheries and Life Science, Dalian Ocean University, Dalian, China.

[3]. Ministry of Education Key Laboratory for Biodiversity Science and Ecological Engineering, Northeast Tiger and Leopard Biodiversity National Observation and Research Station, National Forestry and Grassland Administration Amur Tiger and Amur Leopard Monitoring and Research Center, National Forestry and Grassland Administration Key Laboratory for Conservation Ecology in Northeast Tiger and Leopard National Park, and College of Life Sciences, Beijing Normal University, Beijing 100875, China.

[4]. Ulanqab Branch of the Inner Mongolia Environmental Monitoring Center, Ulanqab, China.

[5]. Chifeng Branch of the Inner Mongolia Environmental Monitoring Center, Chifeng, China.

[*]**Correspondence: yinxuwang@dlou.edu.cn (X. Yin)**

[#] *These authors contributed equally to this work.*

Abstract

Lake salinization is intensifying across arid and semi-arid regions, yet its ecological signal often covaries with lake-specific hydrochemistry and hydrology. We surveyed phytoplankton, zooplankton and water chemistry at 51 sites in four lakes in the Inner Mongolia Autonomous Region, China. The lakes differed markedly in total salts, electrical conductivity, nutrients and organic-matter indicators. Plankton composition, density and taxon diversity also varied among lakes, and Wuliangsu Lake supported the highest mean site-level richness. Models accounting for lake identity revealed limited evidence for consistent within-lake relationships between total salts and phytoplankton or zooplankton richness and Shannon diversity. Cross-trophic density associations showed evidence of among-lake heterogeneity, although this evidence weakened after exclusion of the high-leverage J7 site; no comparable heterogeneity was detected for taxon-richness associations. Pairwise DNCI intervals fell below zero in all phytoplankton comparisons and three zooplankton comparisons, while the three zooplankton comparisons involving JYH overlapped zero. These findings show that plankton variation across the four lakes was associated with contrasting hydrochemical and hydrological settings and heterogeneous cross-trophic numerical associations rather than a single salinity response.

Keywords: phytoplankton; zooplankton; lake hydrochemistry; salinity; community assembly; Inner Mongolia Plateau

Introduction

Climate change and intensified human activity are degrading inland aquatic ecosystems, with salinization and catchment land use emerging as major pressures in arid and semi-arid regions (Herbert et al. 2015; Hintz and Relyea 2019; Ma et al. 2024). The Inner Mongolia Plateau lies within the transition between arid and semi-arid northern China, where annual evaporation reaches 1,200–3,000 mm and precipitation is only 50–450 mm (Geng et al. 2024; Xie et al. 2018). These conditions have produced numerous closed and semi-closed lakes. Their plankton communities sustain material cycling and energy flow: phytoplankton support primary production, whereas zooplankton transfer energy to higher trophic levels (Kiørboe 2011). Plankton composition responds rapidly to environmental change and is widely used to assess lake ecological condition (Carvalho et al. 2013). Regional studies show that lake salinity varies widely across Inner Mongolia and increasingly structures microbial and microeukaryotic distributions (Deng et al. 2024; Liu et al. 2022, 2023). Salinity and nutrients can jointly shape aquatic communities (Tang et al. 2021), while nutrient enrichment can alter phytoplankton biodiversity–function relationships and zooplankton community structure (Chen et al. 2026; Zhu et al. 2026).

Salinity constrains inland-water communities through its effects on organismal physiology, resource availability and trophic interactions (Telesh and Khlebovich 2010; Olli et al. 2023; Stenger-Kovács et al. 2023; Sun et al. 2023). Across natural lakes, however, salinity commonly varies with geography, hydrology and nutrients, and these covariates can produce scale-dependent community patterns (Liu et al. 2022, 2023; Tang et al. 2021). Analyses must therefore distinguish broad among-lake contrasts from relationships expressed within lakes. We

used the four-lake dataset to characterize plankton variation across contrasting hydrochemical settings and to test whether local variation in total salts was consistently associated with plankton diversity after accounting for lake identity.

Phytoplankton and zooplankton communities are structured by interacting environmental and biological filters. In brackish systems, salinity can organize spatial variation in community composition, while water temperature, nutrient availability, seasonality and biotic associations contribute additional variation (Tarafdar et al. 2021). Across saline plateau lakes, zooplankton richness and trophic structure also vary along salinity gradients, but these responses depend on food-chain configuration and temperature (Lin et al. 2017). In shallow lakes, nutrients, conductivity, habitat structure and zooplankton grazing can further modify phytoplankton biomass and diversity (Muylaert et al. 2010; Tolonen et al. 2020). Plankton patterns across lakes should therefore be considered within the broader hydrochemical, hydrological and trophic setting.

Relationships between phytoplankton and zooplankton may vary because salinity, nutrient supply, hydrological confinement, prey composition and food-web structure change together across lakes. Examining matched producer and consumer samples can therefore reveal whether numerical associations are consistent across hydrological settings. Community-assembly theory offers a complementary framework for assessing whether compositional differences are more consistent with dispersal- or niche-related processes (Chase and Myers 2011; Stegen et al. 2013; Zhou and Ning 2017). Studies of microeukaryotic plankton further show that relatively small salinity shifts can alter the balance between assembly processes and network stability (Mo et al. 2021). We therefore evaluated

lake-specific cross-trophic associations and used the dispersal–niche continuum index (DNCI) to compare taxonomic occurrence patterns for each lake pair.

We compared Wuliangsu Lake (WLSH), Juyan Lake (JYH), Daihai Lake (DH) and Dalinor Lake (DLN), which differ in total salts, nutrients, geography and hydrological setting. We asked four questions: (1) how do phytoplankton and zooplankton composition, density, taxon richness and Shannon diversity vary among lakes; (2) are within-lake differences in total salts consistently associated with taxon richness and Shannon diversity after accounting for lake identity; (3) do density and taxon-richness associations between phytoplankton and zooplankton differ among lakes; and (4) how do pairwise DNCI values vary among lake pairs and plankton groups?

Materials and methods

Study area and sampling sites

The study lakes are located in the Inner Mongolia Autonomous Region of northern China, which extends from 97°12′ to 126°04′ E and from 37°24′ to 53°23′ N (Geng et al. 2024). The climate grades from semi-arid in the east to arid in the west, accompanied by declining precipitation and increasing evaporation. Mean annual temperature ranges from −3.2 to 11.5 °C. Annual evaporation is generally 1,200–3,000 mm, whereas annual precipitation is approximately 50–450 mm (Xie et al. 2018; Geng et al. 2024).

Wuliangsu Lake (WLSH). This shallow lake functions as a drainage and water-regulation component of the Hetao Irrigation District. Its water balance and water quality are influenced by irrigation return flow, the main drainage-channel system, direct ecological water

supplementation from the Yellow River and managed discharge. Agricultural drainage and associated nutrient and pollutant inputs are therefore important potential anthropogenic pressures (Wan et al. 2022).

Juyan Lake (JYH). East Juyan Lake is the terminal lake of the endorheic Heihe River Basin. Lake area and water balance depend strongly on regulated river inflow and evaporation. Historical upstream irrigation reduced downstream delivery and contributed to desiccation, whereas the Ecological Water Diversion Project increased inflow and promoted lake recovery; present conditions consequently reflect both arid-basin hydrology and basin-scale water allocation (Zhang et al. 2019).

Daihai Lake (DH). Daihai is a closed inland lake with no natural surface outflow. Its water balance is supplied by precipitation, catchment runoff and groundwater and is dominated on the loss side by evaporation and human water use. Long-term lake recession has been attributed to the joint effects of climate variability and intensified water consumption, including irrigation and groundwater abstraction, making catchment water withdrawal a major potential pressure (Wang et al. 2022).

Dalinor Lake (DLN). Dalinor is an endorheic lake whose recharge includes groundwater and spring-fed rivers; its surface watershed and groundwater basin are not spatially coincident. Hydrogeological evidence identifies southern groundwater and spring-fed rivers as important recharge sources and indicates that warming, drying and increasing human water use may alter the basin water cycle and lake habitat (Li et al. 2021).

Hydrological comparison. The four lakes represent distinct hydrological settings. WLSH is a managed irrigation-drainage and water-regulation system with inflow and controlled discharge.

JYH is a regulated terminal lake sustained by allocated river inflow. DH and DLN are closed endorheic lakes: DH receives precipitation, catchment runoff and groundwater, whereas DLN is strongly influenced by groundwater and spring-fed rivers. Differences in inflow, managed water delivery, surface outflow, evaporation and basin closure can modify flushing, residence time, circulation, salt accumulation and nutrient retention. These contrasts provide the hydrological context for interpreting plankton variation. Because residence time and discharge were not measured during the survey, lake identity was included in the statistical models to represent shared lake-scale conditions.

The locations of the four study lakes are shown in Fig. 1. Samples were collected between 18 August and 6 September 2025 from 51 sites nested within four lakes: JYH (n = 7), WLSH (n = 19), DH (n = 12) and DLN (n = 13). Station identifiers were harmonized across the environmental, phytoplankton and zooplankton datasets before matching. Continuous site-level total salts were retained rather than assigning stations to categorical salinity classes. Table 1 summarizes sampling dates, coordinate ranges and total-salt ranges; complete station records are provided in Supplementary Table S1. The source environmental workbook records J7 within the JYH group, sampled on 27 August 2025 at 101.078984° E, 41.970339° N, with total salts of 499 mg L^{-1}. J7 was 36.7 km from J5, the nearest other recorded JYH station. Because direct hydrological connectivity was not measured, J7 is treated as a geographically separated recorded JYH subsite rather than assumed to represent the same hydrological compartment as J1–J6. It was retained in the primary analyses, and all focal within-lake models were repeated without J7 as a sensitivity analysis.

Basemap data and geographic layers used for the regional context map in Fig. 1A were downloaded from the National Platform for Common Geospatial Information Services (Tianditu; https://www.tianditu.gov.cn/) and assembled in ArcGIS 10.8.2. The regional map was used for geographic context only; no quantitative distances or areas were derived from the displayed basemap. Sampling sites in Fig. 1B and C were plotted from the audited GPS longitude and latitude records in R version 4.5.3 using ggplot2 and maps.

Sampling and laboratory analysis

At each site, dissolved oxygen (DO) and electrical conductivity (EC) were measured 0.5 m below the surface with a WTW Multi 3630 multiparameter meter (WTW, Germany). Water collected at the same depth with a 1.5 L acrylic sampler was transferred to two 500 mL polyethylene bottles and transported to the laboratory. The analytical dataset comprised reported total salts, biochemical oxygen demand (BOD), permanganate index (COD_{Mn}), suspended solids, chemical oxygen demand (COD), total phosphorus (TP), total nitrogen (TN) and ammonia nitrogen (NH_3–N). TP was determined by ammonium molybdate spectrophotometry, TN by alkaline potassium persulfate digestion and ultraviolet spectrophotometry, COD_{Mn} by potassium permanganate titration, and suspended solids gravimetrically after filtration through a 0.7 μm GF/F glass-fiber filter; the remaining determinations followed standard water-analysis procedures (APHA et al. 2017).

Five WLSH BOD observations were reported below the method detection limit of 0.5 mg L^{-1}. For the descriptive summaries in Fig. 2, these left-censored observations were replaced by

one-half of the detection limit (0.25 mg L^{-1}) when calculating lake means and standard errors. BOD was not included in the inferential analyses.

For quantitative phytoplankton analysis, 1 L of water was collected at 0.5 m, fixed immediately with 1.5% Lugol's iodine, sedimented undisturbed for 48 h and concentrated to 100 mL by siphoning the supernatant (Ministry of Ecology and Environment of China 2021, 2023). The concentrate was examined by light microscopy, and taxa were identified to the lowest practicable level following Zhang and Huang (1991). Picophytoplankton was not quantified as a separate size fraction. A separate 64 μm net sample was used only for qualitative morphological verification and was excluded from quantitative analyses. For zooplankton, 50 L of water collected at 0.5 m was filtered through a 64 μm net, concentrated to 50 mL and preserved with 4% formalin (APHA et al. 2017; Zhang and Huang 1991).

Relatively large protozoans retained by the 64 μm mesh were treated as an operational component of the zooplankton dataset. They were identified to the lowest practicable level by light microscopy; testate amoebae followed Ogden and Hedley (1980), and the peritrich ciliate records followed Foissner and Berger (1996). Their densities were adjusted for source and concentrate volumes and expressed as individuals L^{-1}. The included protozoan taxa are listed in Supplementary Table S2.

Each quantitative phytoplankton and zooplankton sample was counted twice, and the arithmetic mean was used in the analyses. Density was calculated as $D = nVc/(VaVs)$, where n is the number counted, Vc is final concentrate volume (mL), Va is the concentrate volume examined (mL), and Vs is original sample volume (L) (Zhang and Huang 1991; Ministry of

189 Ecology and Environment of China 2021, 2023). Phytoplankton and zooplankton densities
190 were expressed as 10^4 cells L^{-1} and individuals L^{-1}, respectively.
191 The source matrices contained 171 phytoplankton and 55 zooplankton operational rows. Of
192 these, 156 phytoplankton units were detected (117 species-level and 39 genus-level), together
193 with 49 non-stage zooplankton units (41 species-level and eight genus-level) and two
194 copepod life-stage bins. Names and spacing were harmonized while genus-level records were
195 retained at their documented resolution. Copepodite and nauplius bins contributed to total
196 zooplankton density, broad-group composition and abundance-based NMDS, but were
197 excluded from taxon richness, Shannon diversity, taxonomic beta diversity and DNCI.
198 Supplementary Table S2 provides the reported and harmonised scientific names, operational
199 taxonomic resolution and occurrence in each lake-associated sampling system for all detected
200 phytoplankton and zooplankton units. Copepodite and nauplius records are identified
201 separately as life-stage categories. Representative light micrographs of selected
202 phytoplankton and zooplankton taxa are provided in Supplementary Fig. S3.
203 Community metrics were calculated at the lowest documented operational taxonomic unit
204 level. Phytoplankton richness and Shannon diversity included all 156 detected units;
205 zooplankton richness and Shannon diversity included the 49 non-stage units. NMDS used the
206 abundance matrices, while taxonomic beta diversity and DNCI used presence–absence
207 matrices without the life-stage bins. Individual taxa were not fitted as model predictors.
208 The revised analyses used density and taxonomic diversity as the community response
209 metrics.

Calculation of plankton indices

Taxonomic diversity

Taxonomic α-diversity was summarized as taxon richness (TR) and the Shannon diversity index (H′). Richness was the number of detected non-stage operational taxonomic units in each sample at the lowest documented identification level; the term taxa is used because species- and genus-level records were combined.

The Shannon diversity index was calculated as follows:

$$H' = -\sum_{i=1}^{S} p_i \ln(p_i)$$

In the formula, S is the number of retained operational taxonomic units in the sample, n_i is the density of the i-th unit, and N is the summed density of all retained units. Copepodite and nauplius bins were excluded from the zooplankton richness and Shannon calculations.

Taxonomic beta-diversity partitioning

Taxonomic beta diversity was calculated separately for phytoplankton and zooplankton from site-by-taxon presence–absence matrices. All pairs of non-empty sites within each lake were compared. Copepodite and nauplius bins were excluded, together with W16 and DL5 because no non-stage zooplankton taxon remained at those sites. Following Baselga (2010), Sørensen total dissimilarity, $\beta_{sor} = (b + c)/(2a + b + c)$, was partitioned into Simpson turnover, $\beta_{sim} = \min(b, c)/(a + \min(b, c))$, and nestedness-resultant dissimilarity, $\beta_{sne} = \beta_{sor} - \beta_{sim}$, where a is the number of shared taxa and b and c are taxa unique to each site. Pairwise distributions and lake medians were summarized descriptively because site pairs were not independent (Soininen et al. 2018; Zheng and Yin 2023).

$$BC_{jk}=\frac{\sum_{i=1}^{S}\left|n_{ij}-n_{ik}\right|}{\sum_{i=1}^{S}\left(n_{ij}+n_{ik}\right)}$$

Statistical analysis

Analyses were conducted in R version 4.5.3 (R Core Team 2026) for 51 sites nested within four lakes. Lake identity was included as a fixed effect in site-level models. Because sampling date was unique to each lake, its effect could not be separated from lake identity. Total salts were converted to g L^{-1} and centered within each lake, and four focal models were fitted for phytoplankton richness, zooplankton richness, phytoplankton Shannon diversity and zooplankton Shannon diversity as response = lake + within-lake-centered total salts. Residual Q–Q and residual-versus-fitted plots, Shapiro–Wilk tests and Breusch–Pagan tests were used as diagnostics. HC3 heteroscedasticity-consistent standard errors were used for coefficient tests and 95% confidence intervals (Long and Ervin 2000). Unstandardized coefficients, robust Wald F statistics with degrees of freedom, exact two-sided P values, model R^2 and sample sizes are reported. For each focal model, leverage, Cook's distance, externally studentized residuals and DFBETAs were examined. The models were then refitted after excluding J7, with within-lake centering recalculated. Lake × centered-total-salts interactions were also tested in the full and J7-excluded datasets to assess whether within-lake slopes were heterogeneous. These interaction analyses were treated as exploratory because only four lakes were sampled and the JYH result was potentially sensitive to J7.

Spatial structure in the residuals of each lake × centered-total-salts model was evaluated using Moran's I. A symmetric two-nearest-neighbour graph was constructed separately within each lake from the GPS coordinates and combined as a block-diagonal, row-standardized weight

matrix. Significance was assessed with 9,999 permutations restricted within lakes, thereby preserving the nested lake membership. A three-nearest-neighbour graph was used as a sensitivity analysis.

Covariation between total salts and TP, TN, COD_{Mn} and COD was summarized using pooled and lake-specific Spearman coefficients. Because the 51 sites were nested within four lakes, pooled coefficients were treated only as descriptive summaries and their nominal P values were not used for inference. Models containing lake identity alone quantified the proportion of variation associated with among-lake differences. Because total salts and nutrients were strongly collinear among lakes, independent lake-level salinity and nutrient coefficients were not estimated.

Non-metric multidimensional scaling (NMDS) was performed separately for phytoplankton and zooplankton using site-by-taxon density matrices. Bray–Curtis dissimilarity was calculated between sites with vegan version 2.7-2; it ranges from 0 for identical taxon-density composition to 1 for complete dissimilarity (Bray and Curtis 1957; Oksanen et al. 2025). NMDS was then used to provide a descriptive ordination of community composition (Kruskal 1964). Multivariate location was summarized with adonis2 using zero permutations, yielding descriptive pseudo-F and R^2 values without a permutation P value (Anderson 2001). Multivariate dispersion was evaluated as distance to the spatial median with bias-adjusted betadisper, followed by a 999-permutation PERMDISP test (random seed 20260927; Anderson 2006). The ordination and dispersion statistics describe site-level compositional structure within the four sampled lakes.

Cross-trophic associations were evaluated at the 51 matched sites using two complementary responses. Density was analyzed as $\log_{10}$(zooplankton density) = lake × within-lake-centered $\log_{10}$(phytoplankton density), and richness as zooplankton taxon richness = lake × within-lake-centered phytoplankton taxon richness. Additive models estimated a common within-lake slope, and the three interaction terms jointly tested whether slopes differed among lakes. HC3 standard errors and Wald F tests were used throughout. Lake-specific slopes were then estimated for interpretation. Because J7 had unusually low total salts within JYH and was geographically separated from the other JYH sites, both interaction tests were repeated after excluding J7. These analyses quantified contemporaneous numerical covariation between trophic levels.

DNCI-based community-assembly analysis

The dispersal–niche continuum index (DNCI) was used to assess the relative contribution of dispersal- and niche-related processes to taxonomic community assembly (Vilmi et al. 2021). DNCI was calculated with DNCImper version 0.0.1.7000 (Gibert and Escarguel 2025) from site-by-taxon presence–absence matrices, separately for phytoplankton and zooplankton. All six lake pairs were analyzed. For each comparison, the larger group was randomly subsampled to match the smaller group, and the analysis was repeated 20 times with 50 permutations per repeat (random seed 20260925). Copepodite and nauplius bins were excluded from the zooplankton matrix, together with W16 and DL5 because no non-stage zooplankton taxon remained at those sites. Median DNCI was reported for each lake pair. A method-specific confidence interval below zero indicated greater support for dispersal-related processes, an

interval above zero indicated greater support for niche-related processes, and an interval overlapping zero was considered inconclusive.

Figures were generated with ggplot2 version 4.0.3 (Wickham 2016), assembled with patchwork version 1.3.2 (Pedersen 2025) and exported with ragg version 1.5.0 (Pedersen and Shemanarev 2025).

Results

Spatial variation in hydrochemistry

Nutrients and other hydrochemical variables differed markedly among lakes (Fig. 2). Site-level total salts ranged from 832 to 1,501 mg L^{-1} in WLSH, 499 to 4,530 mg L^{-1} in JYH, 7,990 to 8,960 mg L^{-1} in DH and 7,990 to 9,780 mg L^{-1} in DLN (Table 1; Supplementary Table S1); corresponding means were 997, 3,731, 8,571 and 8,952 mg L^{-1}. The partial overlap between JYH and WLSH further illustrates the absence of four discrete salinity classes. Pooled Spearman coefficients summarized among-lake covariation between total salts and TP (r_s = 0.784), TN (0.731), COD_{Mn} (0.879) and COD (0.838; Fig. 3). Lake identity explained 99.9%, 98.4%, 98.3% and 98.5% of the variation in these variables, respectively. Within-lake correlations were weaker and varied in direction, showing that the pooled relationships arose largely from separation among lakes. Mean TN and TP were 1.105 and 0.031 mg L^{-1} in WLSH, 0.569 and 0.066 mg L^{-1} in JYH, 2.438 and 0.060 mg L^{-1} in DH, and 5.099 and 2.251 mg L^{-1} in DLN. Thus, DLN had the highest mean concentrations of both nutrients, whereas TN and TP followed different among-lake rankings elsewhere.

Exploratory within-lake associations with total salts

HC3-robust tests of within-lake-centered total salts are reported in Table 2. The 95% confidence intervals for all four retained responses—phytoplankton richness, zooplankton richness, phytoplankton Shannon diversity and zooplankton Shannon diversity—included zero. Thus, the survey provided limited evidence for a consistent within-lake association between total salts and these taxonomic diversity metrics after adjustment for lake identity. J7 had leverage of 0.778 in each model. For phytoplankton richness, zooplankton richness, phytoplankton Shannon diversity and zooplankton Shannon diversity, respectively, Cook's distances were 0.205, 1.057, 0.054 and 0.021; externally studentized residuals were −0.536, 1.234, −0.274 and 0.171; and the largest absolute DFBETAs were 0.907, 2.089, 0.464 and 0.289. After J7 was excluded, the common within-lake slopes were −0.563 (95% CI −4.541 to 3.414), 0.586 (−0.526 to 1.699), 0.081 (−0.437 to 0.598) and 0.100 (−0.306 to 0.506), respectively; all confidence intervals still included zero (Table 2). The joint lake × total-salts tests were non-significant for all four responses in the full dataset (P = 0.9220, 0.8844, 0.9846 and 0.6004), but after J7 was excluded they were significant for zooplankton richness (P = 0.0192) and zooplankton Shannon diversity (P = 0.0076), while remaining non-significant for both phytoplankton responses (P = 0.7626 and 0.9845). Thus, the common-slope conclusion was unchanged, whereas exploratory evidence for among-lake heterogeneity in zooplankton slopes was sensitive to J7.

Lake-specific slopes from the full lake × total-salts models were imprecise and differed in direction. Expressed per 1 g L^{-1} increase in within-lake-centered total salts, phytoplankton-richness slopes were −2.296 (HC3 95% CI −107.254 to 102.661) in WLSH,

0.830 (−27.073 to 28.734) in JYH, 0.223 (−2.324 to 2.769) in DLN and 1.785 (−1.985 to 5.554) in DH. Zooplankton-richness slopes were −0.292 (−19.482 to 18.897), −1.378 (−10.967 to 8.211), 0.736 (−0.474 to 1.946) and −0.229 (−2.769 to 2.311), respectively. Phytoplankton-Shannon slopes were 0.170 (−6.364 to 6.704), 0.155 (−0.504 to 0.814), 0.167 (−0.515 to 0.849) and −0.059 (−1.090 to 0.973), and zooplankton-Shannon slopes were 1.305 (−0.901 to 3.511), 0.088 (−2.708 to 2.884), −0.093 (−0.422 to 0.237) and −0.254 (−0.923 to 0.414). In the full dataset, joint lake × total-salts tests did not support slope heterogeneity for phytoplankton richness ($F(3, 43) = 0.161$, $P = 0.9220$), zooplankton richness ($F(3, 43) = 0.217$, $P = 0.8844$), phytoplankton Shannon diversity ($F(3, 43) = 0.051$, $P = 0.9846$) or zooplankton Shannon diversity ($F(3, 43) = 0.629$, $P = 0.6004$). The wide intervals reflected the narrow and non-overlapping salinity ranges within several lakes.

Residual Moran tests for the full interaction models found no spatial autocorrelation for phytoplankton richness (two-neighbour $I = 0.097$, permutation $P = 0.3723$; three-neighbour $I = −0.095$, $P = 0.8454$) or phytoplankton Shannon diversity ($I = 0.068$, $P = 0.2930$; $I = 0.015$, $P = 0.3873$). Positive residual spatial autocorrelation remained for zooplankton richness ($I = 0.307$, $P = 0.0268$; $I = 0.320$, $P = 0.0038$) and zooplankton Shannon diversity ($I = 0.214$, $P = 0.0172$; $I = 0.117$, $P = 0.0301$). Accordingly, the zooplankton slope estimates are treated as exploratory because HC3 standard errors address heteroscedasticity but not residual spatial dependence.

355 **Plankton community structure**

356 Phytoplankton composition varied markedly among lakes. Seven major groups were recorded:
357 Cyanobacteria, Cryptophyta, Xanthophyta, Bacillariophyta, Dinophyta, Euglenophyta and
358 Chlorophyta. WLSH had the highest taxon richness, whereas richness was lower in JYH, DH
359 and DLN. Chlorophyta and Xanthophyta made large contributions across lakes, while several
360 minor groups, including Dinophyta and Euglenophyta, occurred mainly in WLSH. Dominant
361 taxa also varied among lakes. *Cyclotella meneghiniana* and *Microcystis* spp. were abundant in
362 lakes with lower total salts, whereas *Ankistrodesmus* and *Cryptomonas* occurred primarily in
363 WLSH and JYH. Fig. S1 summarizes major-group taxon richness for both plankton
364 communities.

365 Zooplankton composition also varied among lakes. Rotifera was the dominant taxonomic
366 group and accounted for most non-stage taxa, while WLSH supported the highest zooplankton
367 richness. Large, net-retained protozoans occurred mainly in WLSH and at individual sites in
368 JYH, DH and DLN. Copepod-related records were proportionally more prominent in DH and
369 DLN, which had the highest total-salt ranges. Copepodite and nauplius records were retained as
370 life-stage bins rather than independent taxa. Fig. 4 summarizes broad taxonomic-group
371 composition.

372 NMDS revealed partly differentiated but overlapping site clouds among lakes (Fig. 5), with
373 stress values of 0.161 for phytoplankton and 0.112 for zooplankton. Descriptive adonis2
374 partitioning attributed $R^2 = 0.259$ to lake identity for phytoplankton (pseudo-$F(3, 47) = 5.468$)
375 and $R^2 = 0.332$ for zooplankton (pseudo-$F(3, 47) = 7.775$). PERMDISP detected heterogeneous

dispersion for phytoplankton ($F(3, 47) = 5.438$, $P = 0.002$) and zooplankton ($F(3, 47) = 9.186$, $P = 0.001$; Table 3). Mean distances to the group median were 0.587, 0.610, 0.648 and 0.358 for phytoplankton and 0.388, 0.456, 0.188 and 0.201 for zooplankton in WLSH, JYH, DLN and DH, respectively. The ordinations therefore capture both compositional location and within-lake dispersion.

Plankton density

Phytoplankton density differed markedly among lakes. Cryptophyta dominated phytoplankton density in WLSH and accounted for nearly all recorded cells in DLN, whereas Bacillariophyta dominated in DH. JYH had a relatively high contribution from Cyanobacteria and the lowest mean total phytoplankton density (Fig. 4A).

Zooplankton density composition also differed among lakes. Rotifera contributed most of the density in WLSH, whereas Copepoda dominated in JYH, DLN and DH. Cladocera occurred in JYH, DLN and DH. Mean total zooplankton density was highest in DH and lowest in JYH (Fig. 4B).

Plankton taxonomic diversity

Taxonomic α-diversity varied among lakes. WLSH had the highest mean site-level richness for both phytoplankton (22.2 taxa) and zooplankton (8.6 taxa), whereas mean richness was lower in JYH, DLN and DH (Fig. 6).

Within-lake pairwise Sørensen dissimilarity was high for phytoplankton in all four lakes. Median total dissimilarity was 0.730 in WLSH, 0.818 in JYH, 0.817 in DLN and 0.732 in DH, with turnover generally contributing the larger component.

Zooplankton also showed substantial within-lake taxonomic dissimilarity. Median total Sørensen dissimilarity was 0.625 in WLSH, 1.000 in JYH, 0.800 in DLN and 0.667 in DH, and the relative contributions of turnover and nestedness varied among lakes (Fig. S2).

Cross-trophic associations

After adjustment for lake identity, the common within-lake density slope was small and uncertain (slope = 0.096; HC3 95% CI = −0.216 to 0.408; $F(1, 46) = 0.383$; $P = 0.5393$; model $R^2 = 0.229$; $n = 51$). Slopes nevertheless differed among lakes (joint interaction $F(3, 43) = 5.828$; $P = 0.0020$; Fig. 7A): WLSH, 0.506 (95% CI = −0.400 to 1.412; $P = 0.2552$); JYH, −1.459 (−2.415 to −0.503; $P = 0.0112$); DLN, 0.007 (−0.105 to 0.118; $P = 0.8975$); and DH, 0.099 (−0.164 to 0.362; $P = 0.4219$). After J7 was excluded, the interaction weakened but remained at the conventional significance threshold ($F(3, 42) = 2.838$; $P = 0.0494$), and the JYH slope was no longer significant (slope = −1.168; 95% CI = −2.439 to 0.103; $P = 0.0633$). The common richness slope also included zero (slope = 0.075; HC3 95% CI = −0.181 to 0.332; $F(1, 46) = 0.348$; $P = 0.5580$; model $R^2 = 0.485$), and richness slopes did not differ among lakes (joint interaction $F(3, 43) = 0.746$; $P = 0.5308$; Fig. 7B).

Pairwise DNCI patterns

Median DNCI values were negative for all six lake pairs in both plankton groups (Fig. 8; Table 4). For phytoplankton, the reported intervals were entirely below zero for all six lake pairs. For zooplankton, the intervals were entirely below zero for WLSH–DLN, WLSH–DH and DLN–DH, whereas those for WLSH–JYH, JYH–DLN and JYH–DH included zero. Each DNCI estimate was calculated as the median of 20 balanced resampling runs, with 50

418 permutations per run. The balanced sample sizes and corresponding intervals are provided in
419 Table 4.

420 Discussion

421 Hydrochemical context and taxonomic patterns

422 The four lakes formed distinct hydrochemical clusters in total salts, conductivity, nutrients and
423 organic-matter indicators (Figs. 2 and 3). Strong pooled correlations between total salts and TP,
424 TN, COD_{Mn} and COD arose mainly from separation among these clusters, whereas within-lake
425 relationships were weaker and varied in direction. This scale dependence shows that
426 lake-specific hydrochemistry provides a more appropriate framework than a single salinity
427 gradient. Hydrological setting offers a plausible organizing mechanism because inflow, basin
428 closure and water management influence salt accumulation, nutrient retention and circulation
429 in arid-basin lakes (Herbert et al. 2015; Williams 1999; Wurtsbaugh et al. 2017;
430 Cunillera-Montcusí et al. 2022). Remote-sensing analyses also document pronounced salinity
431 variation among Inner Mongolian lakes (Deng et al. 2024). WLSH receives irrigation drainage
432 and managed ecological supplementation, JYH depends on regulated basin inflow, DH has
433 experienced substantial water loss, and DLN is sensitive to groundwater recharge and
434 increasing basin water use (Wan et al. 2022; Li et al. 2021; Wang et al. 2022; Zhang et al. 2019).
435 The partly overlapping NMDS configurations and heterogeneous multivariate dispersion
436 further indicate substantial spatial structure within lakes as well as compositional differences
437 among them.

Lake-specific salinity slopes varied in sign and had wide confidence intervals, while the full-data interaction tests did not detect slope heterogeneity. The uncertainty was greatest where within-lake salinity ranges were narrow. Residual spatial autocorrelation in the zooplankton models further suggests that local habitat configuration or unmeasured spatial processes contributed to site-level variation.

The hydrological contrasts also clarify why lake means did not form a simple biological sequence with increasing total salts. Irrigation drainage and managed water delivery in WLSH can introduce nutrients while maintaining water exchange, whereas regulated inflow controls both water level and connectivity in JYH. In the closed DH and DLN basins, evaporative concentration can increase dissolved salts, but nutrient accumulation also depends on groundwater inputs, catchment loading, sediment exchange and biological retention. Salinity therefore integrates part of the water-balance history without representing all processes that determine nutrient supply or plankton habitat. Interpreting the four systems as distinct hydrochemical settings accommodates these multiple pathways and is consistent with broader evidence from salinizing inland waters (Cunillera-Montcusí et al. 2022; Wurtsbaugh et al. 2017).

The observed among-lake differences are consistent with the broader environmental filtering of plankton communities reported in other aquatic systems. In a tropical brackish lagoon, salinity was a major correlate of phytoplankton composition, but temperature, seasonality and biotic associations also contributed to community variation (Tarafdar et al. 2021). Similarly, zooplankton richness and trophic configuration changed along a broad salinity gradient in Tibetan lakes, with responses varying according to food-chain structure (Lin et al. 2017).

Nutrient availability, conductivity, habitat characteristics and grazing can further influence phytoplankton–zooplankton relationships (Muylaert et al. 2010; Tolonen et al. 2020). In the present study, total salts covaried with nutrients, organic-matter indicators and lake-specific hydrological conditions. The plankton patterns are therefore interpreted as responses to the combined environmental setting of each lake, with salinity representing one component of this setting.

The TN and TP distributions illustrate this coupled hydrochemical context. DLN had the highest mean TN (5.099 mg L^{-1}) and TP (2.251 mg L^{-1}), together with the highest COD_{Mn} (26.862 mg L^{-1}) and COD (205.615 mg L^{-1}). This co-occurrence is consistent with nutrient and organic-matter retention under weak flushing, strong evaporation and endorheic confinement. Mineralization, salinization and sediment release can further recycle or mobilize accumulated phosphorus (Gardolinski et al. 2004; Søndergaard et al. 2007; van Diggelen et al. 2014). The pattern nevertheless differed between elements: DH had elevated TN (2.438 mg L^{-1}) and COD (103.167 mg L^{-1}), while TP was similar to JYH (0.060 versus 0.066 mg L^{-1}). Nitrogen and phosphorus may therefore differ in their sources, retention, sediment interactions and biological uptake, with consequences that vary among phytoplankton, zooplankton and fish communities (Chen et al. 2026; Zhang et al. 2025; Zhu et al. 2026). Direct evaluation of these mechanisms would require organic-carbon measurements, sediment nutrient pools, external loading estimates and water-exchange data.

Total nutrient concentrations integrate dissolved and particulate pools and therefore reflect both external supply and internal recycling. The simultaneous elevation of TN, TP and oxygen-demand indicators in DLN is compatible with the retention of nutrient-rich organic

material, followed by mineralization and sediment–water exchange. DH, by contrast, combined elevated TN and COD with comparatively modest TP, suggesting that nitrogen and phosphorus were regulated by different source, retention or uptake pathways. Such element-specific behavior can alter phytoplankton composition and food quality even when total salinity is similar, as reported for plateau lakes exposed to interacting climatic and nutrient stressors (Gu et al. 2024). Nutrient enrichment may then propagate differently through phytoplankton, zooplankton and fish assemblages and reorganize food-web structure (King et al. 2024; Chen et al. 2026; Zhang et al. 2025; Zhu et al. 2026).

Heterogeneous cross-trophic associations and study contribution

Exploratory analyses suggested that cross-trophic density associations may differ among lakes. The interaction was driven mainly by a negative JYH slope, whereas slopes in the other lakes were weak or positive. However, the JYH estimate was based on only seven sites, and both the overall interaction and the JYH-specific association weakened after excluding J7. These findings provide tentative evidence of heterogeneous numerical associations between phytoplankton and zooplankton across lakes, but their robustness and ecological basis remain uncertain.

Density describes numerical standing stocks rather than prey biomass, food quality, grazing or energy transfer. Variation in cell or body size, taxonomic composition, reproduction, mortality, predation and temporal lags can all alter the relationship between phytoplankton and zooplankton counts. The absence of a common richness association likewise indicates that producer and consumer taxon numbers did not covary consistently within lakes during this

survey. Seasonal sampling, size-resolved biomass measured with documented conversions, grazing experiments and hydrological observations will be needed to determine whether the lake-specific numerical patterns reflect trophic interactions or shared responses to environmental conditions (King et al. 2024; Chen et al. 2026).

Interpretation of DNCI patterns

Pairwise DNCI values provided a comparative summary of taxonomic occurrence patterns among lakes. Intervals were below zero for all phytoplankton pairs and three zooplankton pairs, whereas the three zooplankton comparisons involving JYH overlapped zero. Under the DNCI framework, intervals below zero are consistent with a greater relative contribution of dispersal-related processes (Vellend 2010; Chase and Myers 2011; Vilmi et al. 2021). These occurrence-based comparisons do not identify hydrological connections, dispersal limitation or a specific assembly mechanism. We therefore interpret the DNCI results together with beta-diversity patterns as comparative evidence of heterogeneity among lake pairs.

The contrast between plankton groups lay in the consistency of their DNCI estimates. All phytoplankton intervals remained below zero, whereas the three zooplankton comparisons involving JYH overlapped zero. Thus, the pairwise DNCI pattern was more consistent for phytoplankton than for zooplankton across the sampled lakes. The ecological causes of this contrast require direct information on connectivity, dispersal and temporal dynamics. Turnover, nestedness and DNCI together provide complementary descriptions of taxonomic composition across the four hydrochemically distinct lakes (Vellend 2010; Vilmi et al. 2021; Zheng and Yin 2023).

Study limitations and future perspectives

This study compared phytoplankton and zooplankton across four hydrochemically contrasting lakes during a single late-summer survey. Hydrology, nutrient status, geography and sampling date varied among lakes, so the observed patterns represent coupled lake-specific gradients within one seasonal window, and causal inference is constrained by this observational cross-sectional design. Near-surface sampling represented one depth stratum, and the 64 μm mesh emphasized larger protozoans and copepod stages. Community abundance analyses were based on organism count-derived density data, while taxonomic beta-diversity and DNCI analyses used presence–absence matrices; no measured biovolume or biomass data were used. Numerical density therefore cannot be directly equated to biomass, prey availability, grazing intensity or energy-transfer processes. Juyan Lake (JYH) had a limited sample size (n = 7), and the geographically separated J7 station influenced zooplankton interaction tests and the JYH-specific cross-trophic density slope. Hydrological connectivity between J7 and the other JYH stations was not independently verified; therefore, its recorded lake assignment should not be interpreted as evidence of shared hydrological conditions. Accordingly, cross-trophic patterns for JYH should be treated as exploratory and should not be over-generalized. Residual spatial autocorrelation in the zooplankton diversity models further indicated spatial structure beyond the measured variables, and HC3 heteroscedasticity-consistent standard errors do not correct for such spatial dependence. These features define the temporal, spatial, taxonomic and inferential scope of the study.

Future research should combine seasonal and depth-resolved sampling with a larger set of lakes spanning overlapping ranges of salinity, nutrient status and hydrological confinement. Direct

546 measurements of inflow and outflow, residence time, water-level fluctuation, mixing,
547 groundwater exchange, external nutrient loading and sediment nutrient fluxes would allow
548 hydrological and biogeochemical pathways to be evaluated explicitly. Whole-water
549 enumeration or complementary fine-mesh sampling would improve coverage of small
550 protozoans and early copepod stages. Standardized measurements of organism dimensions,
551 biovolume, wet and dry mass, carbon conversion, grazing and prey quality would support
552 analyses of producer–consumer interactions. Long-term observations, targeted experiments
553 and hierarchical models that account for sites nested within lakes could evaluate how
554 salinization, nutrient enrichment and connectivity covary with temporal changes in plankton
555 communities.

556 ## Conclusions

557 The four lakes differed markedly in hydrochemistry, plankton composition, density and taxon
558 diversity. Total salts covaried with nutrients, conductivity and organic-matter indicators, and
559 lake identity accounted for most of this variation. Within-lake coefficients for all four
560 taxonomic diversity metrics were uncertain. Exploratory analyses suggested heterogeneity in
561 cross-trophic density associations among lakes, although the interaction weakened after
562 excluding the geographically separated J7 site. In contrast, there was no clear statistical
563 evidence of among-lake differences in cross-trophic taxon-richness slopes. DNCI intervals
564 were below zero in all phytoplankton comparisons and three zooplankton comparisons,
565 whereas the three zooplankton comparisons involving JYH overlapped zero. The observed
566 plankton patterns were associated with lake-specific hydrochemistry, hydrological setting,
567 taxonomic turnover and heterogeneous cross-trophic numerical associations. Seasonal surveys

integrating water exchange, nutrient loading, grazing and standardized biomass measurements will help resolve the underlying mechanisms.

Acknowledgements

We thank S. Zhang, Y. Liu, X. Liu and Y. Song for technical assistance during the field survey.

Author contributions

Y.Z., W.L. and J.Z. contributed equally to this work. Y.Z., W.L., J.Z., Z.W., P.H., Y.T., X.Z., H.L., J.Q., R.W. and X.Y. conceived the study. Y.Z., W.L., P.H. and Z.W. analyzed the data. X.Y., Y.T. and J.Z. designed the statistical framework and extended the analyses. W.L., J.Z., Z.W., P.H. and Y.Z. drafted the manuscript. All authors reviewed and edited the manuscript.

Declarations

Funding

This work was supported by the Key Project of the Natural Science Foundation of Inner Mongolia Autonomous Region, “Key technology research and application demonstration of lake aquatic ecological quality evaluation in Inner Mongolia” (2024ZD13).

Competing interests

The authors declare no competing interests.

Ethics approval

Not applicable.

Consent to participate

Not applicable.

Consent for publication

Not applicable.

Data availability

The data supporting this study are available from the corresponding author upon reasonable request.

Figure captions

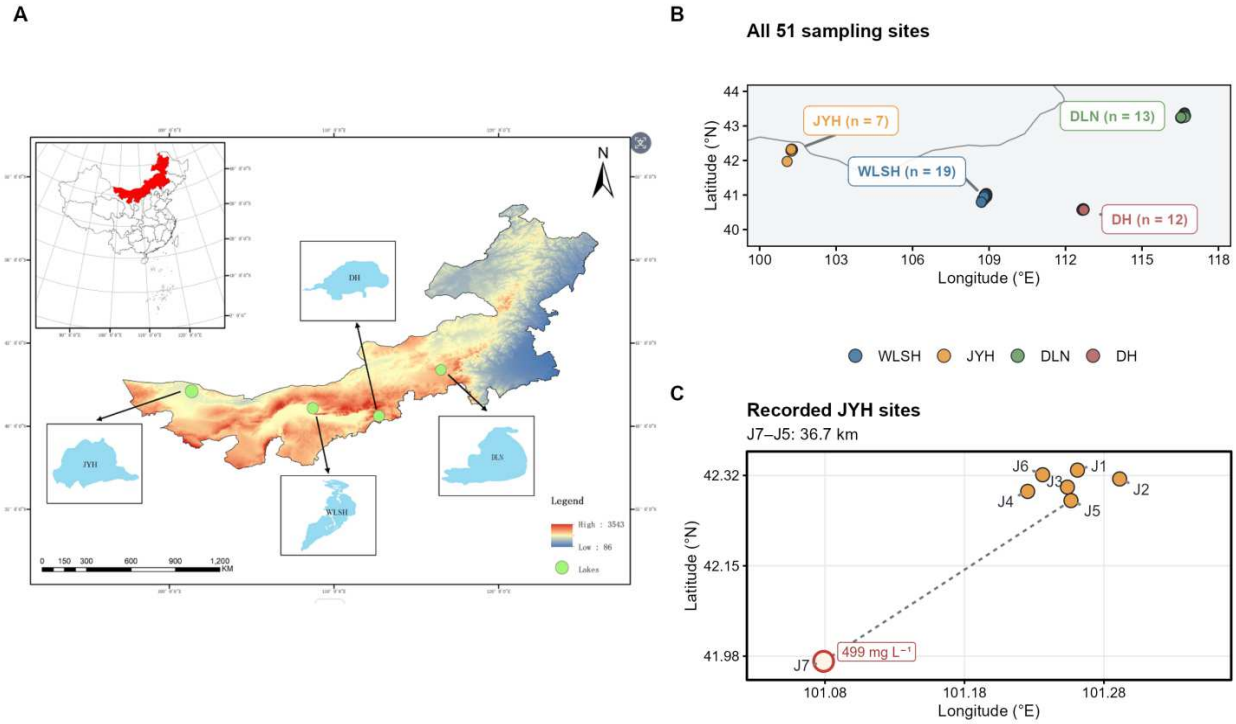


Fig. 1 Geographic context and sampling-site locations. (A) Regional geographic context showing the locations of the four study lakes in northern China. (B) All 51 sampling sites, colored by recorded lake group. (C) The seven recorded JYH sites; J7 is highlighted and labelled with its measured total salts (499 mg L^{-1}), and the dashed line connects it to J5, the nearest other recorded JYH station (36.7 km). Coordinates and sampling metadata were taken from the audited environmental workbook. Panels B and C were generated in R version 4.5.3 using ggplot2 and maps. Basemap data and geographic layers in panel A were downloaded from the National Platform for Common Geospatial Information Services

(Tianditu; https://www.tianditu.gov.cn/), and the regional map was prepared in ArcGIS 10.8.2

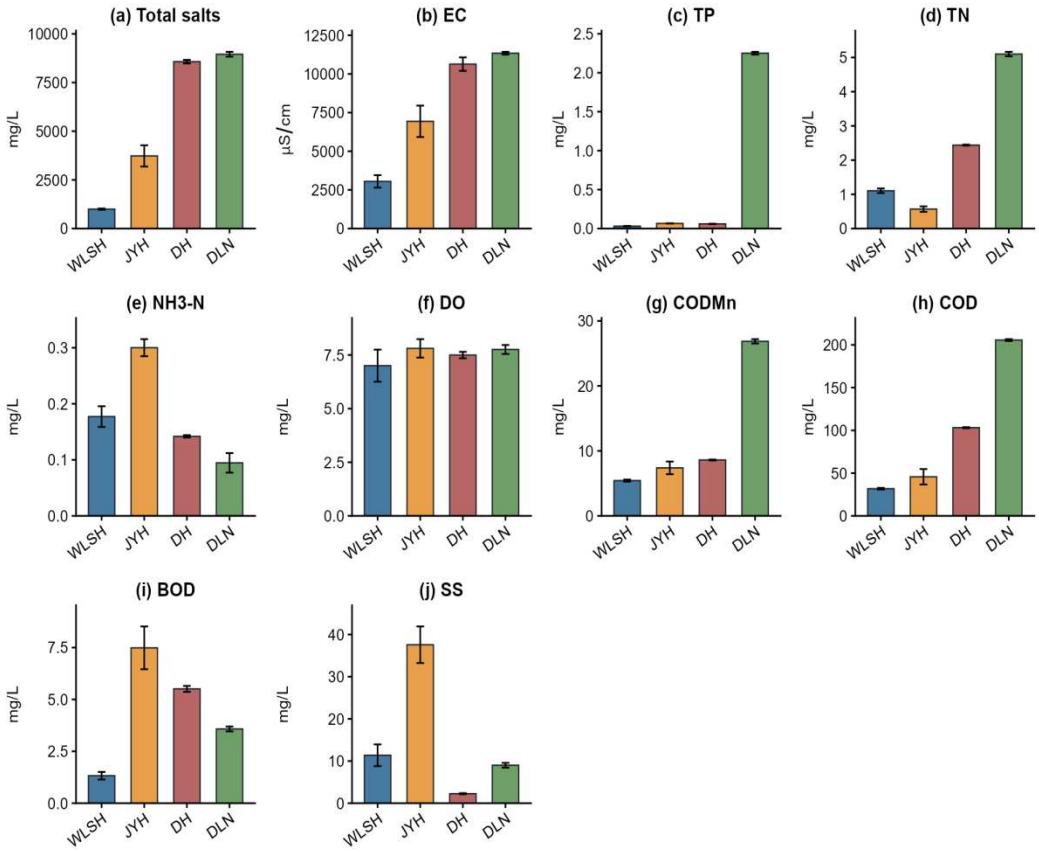


Fig. 2 Variation in ten audited water-quality variables among the four study lakes: total salts, electrical conductivity (EC), total phosphorus (TP), total nitrogen (TN), ammonia nitrogen (NH_3–N), dissolved oxygen (DO), permanganate index (COD_{Mn}), chemical oxygen demand (COD), biochemical oxygen demand (BOD) and suspended solids (SS). Bars show lake means, and error bars show standard errors across sites. Five WLSH BOD records were reported as "0.5L", where "L" denotes a result below the 0.5 mg L^{-1} method detection limit. For both the plotted mean and standard error, these five records were replaced by one-half of the detection limit (0.25 mg L^{-1}). BOD was not used in inferential models. Lakes are ordered by increasing mean total salts: WLSH, JYH, DH and DLN.

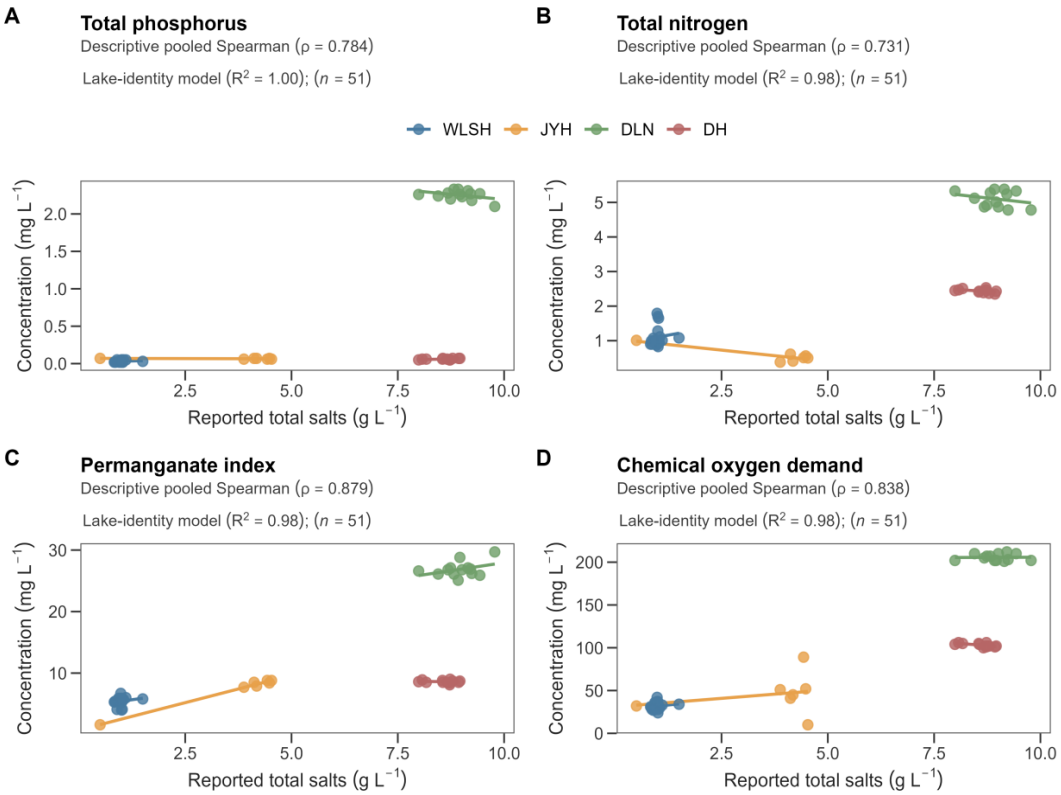
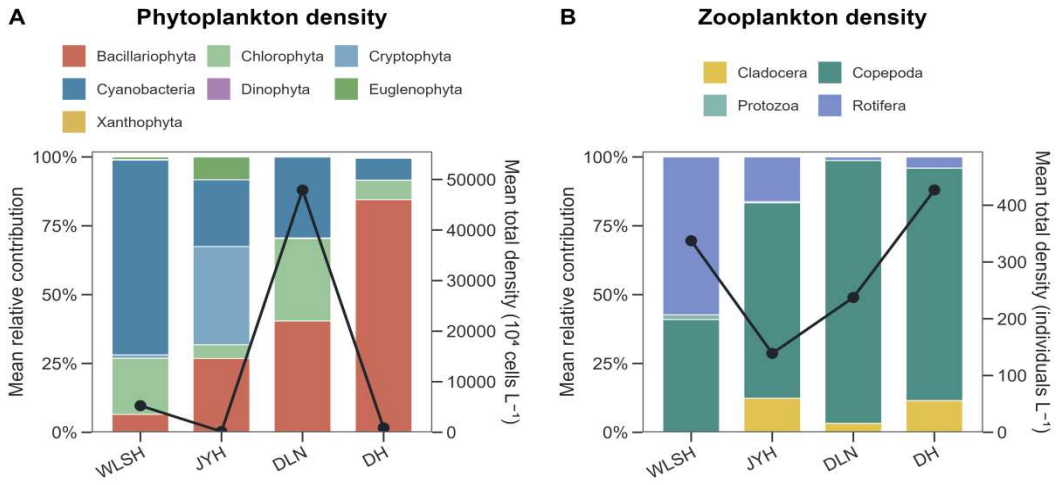
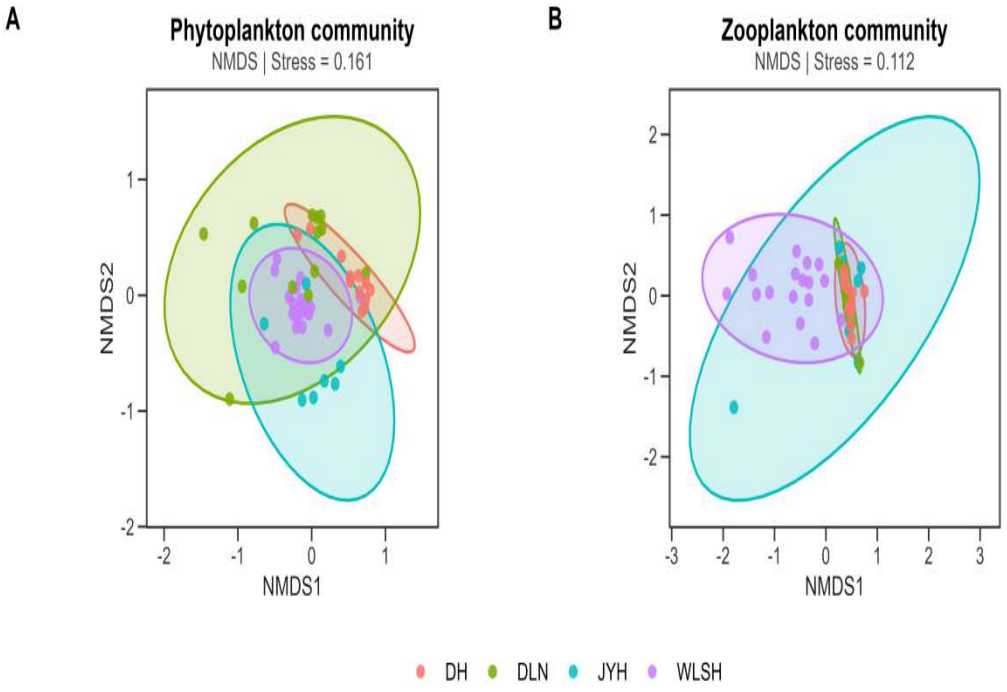


Fig. 3 Descriptive covariation between total salts and (A) total phosphorus, (B) total nitrogen, (C) permanganate index and (D) chemical oxygen demand across 51 sites in four lakes. Points represent sampling sites, and colored lines show lake-specific least-squares fits where estimable. Pooled Spearman coefficients are retained only as descriptive summaries; inferential P values are omitted because sites are nested within lakes. The displayed R^2 values quantify variation associated with the lake-identity model.



619

620 Fig. 4 Taxonomic-group composition and mean total density of phytoplankton and zooplankton across
621 the four lakes. Stacked bars show the mean site-level relative contribution of each group, and black
622 points and lines show lake means. (A) Phytoplankton density (10^4 cells L^{-1}). (B) Zooplankton density
623 (individuals L^{-1}).



624

625 Fig. 5 Non-metric multidimensional scaling (NMDS) ordination of (A) phytoplankton and (B)
626 zooplankton composition across the four lakes. Points represent sampling sites, colors denote lakes, and
627 shaded polygons show 95% normal-theory data ellipses for each lake. Stress values are shown above
628 each panel. The ellipses are descriptive and should be interpreted together with the PERMDISP results in
629 Table 3.

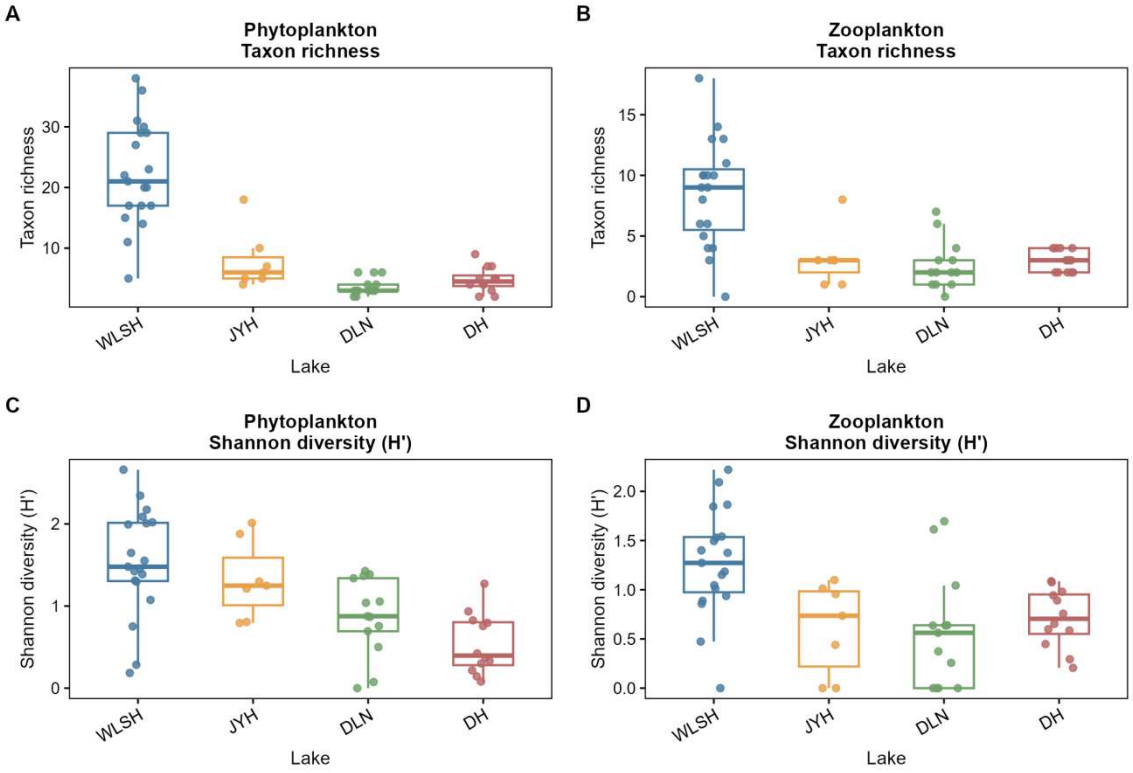


Fig. 6 Site-level taxonomic α-diversity of phytoplankton and zooplankton across the four lakes. Copepodite and nauplius life-stage bins were excluded from zooplankton richness and Shannon diversity. Points represent sites; boxes show medians and interquartile ranges.

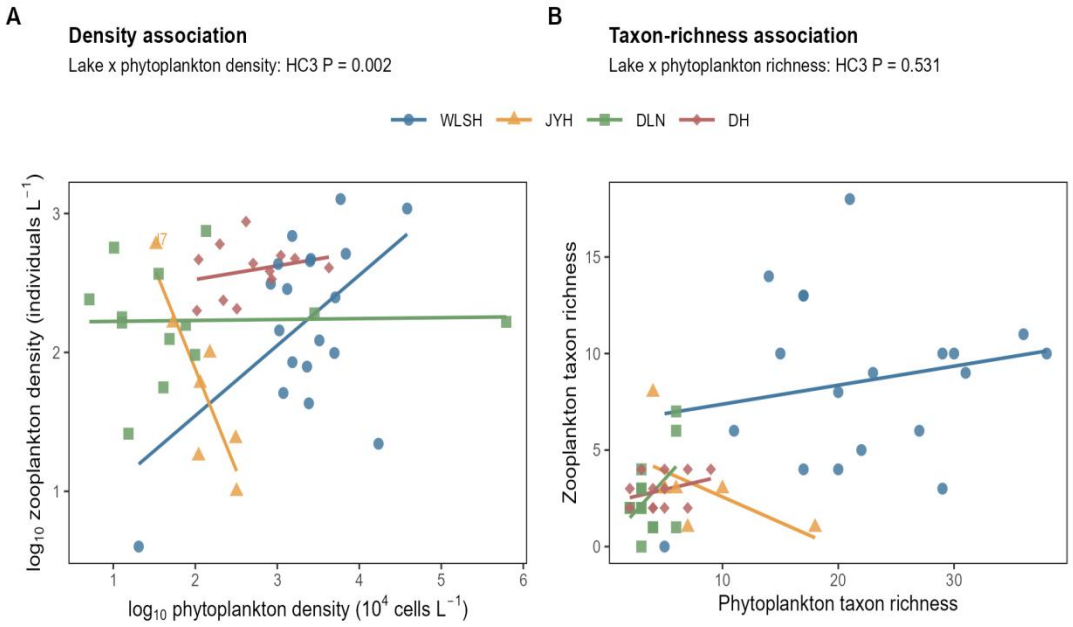


Fig. 7 Cross-trophic density and taxon-richness associations across 51 matched sites. Lines show separate least-squares fits for each lake; colors and symbols identify lakes. (A) Log_{10}-transformed phytoplankton and zooplankton density; J7 is labelled because it had high leverage within JYH. (B) Phytoplankton and zooplankton taxon richness. Panel annotations report HC3 joint tests of the lake × phytoplankton interaction. The panels represent contemporaneous numerical covariation.

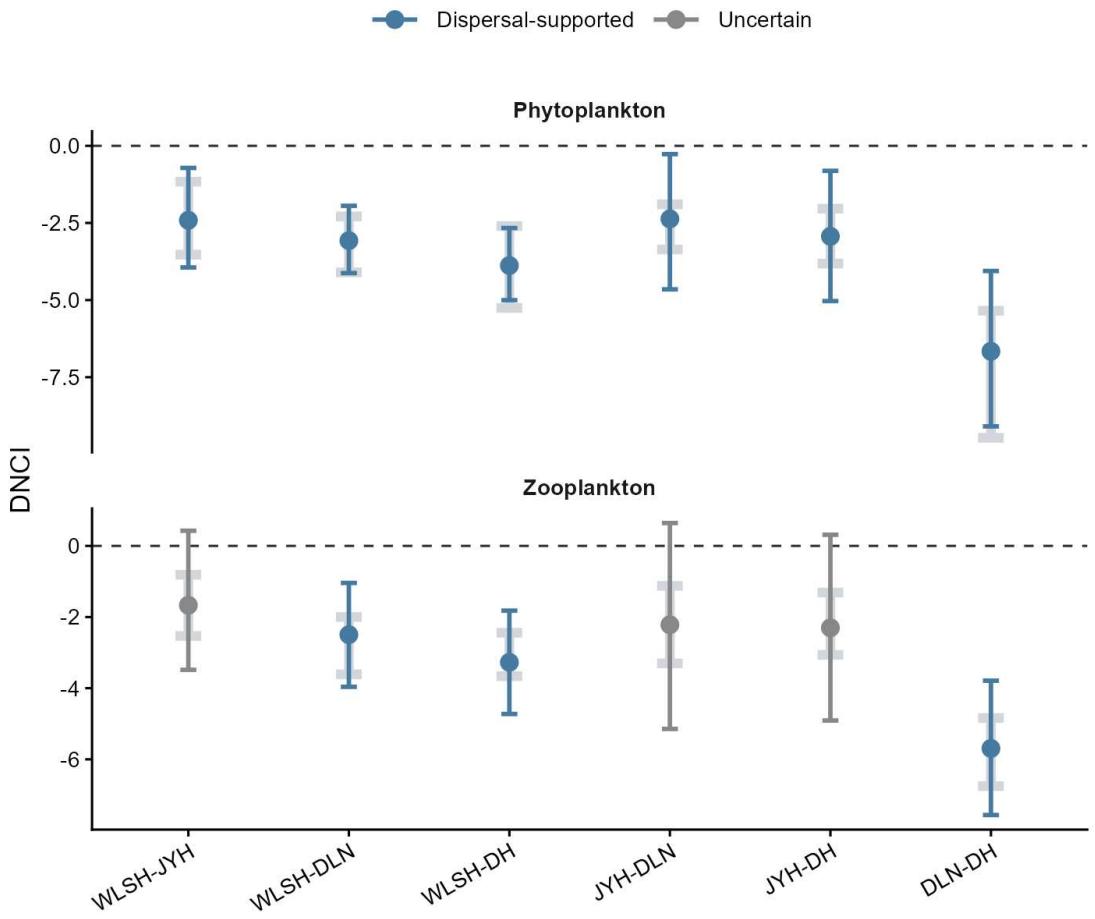


Fig. 8 Pairwise dispersal–niche continuum index (DNCI) for phytoplankton and zooplankton communities. Points show median DNCI across 20 balanced resampling runs. Thick colored intervals show median method-specific confidence intervals, and pale gray intervals show the 2.5th–97.5th percentile range across runs. Intervals entirely below zero support a greater relative contribution of dispersal-related processes; intervals overlapping zero are inconclusive. Each run used 50 permutations.

630

Tables

Table 1 Sampling coverage, sampling dates, coordinate ranges and site-level reported total-salt ranges for the four lakes

Lake	Sites	Sampling dates	Longitude (°E)	Latitude (°N)	Reported total salts (mg L^{-1}; g L^{-1})
WLSH	19	1–6 Sep 2025	108.695600–108.913600	40.790192–41.039015	832–1,501 (0.832–1.501 g L^{-1})
JYH	7	27 Aug 2025	101.078984–101.291244	41.970339–42.330025	499–4,530 (0.499–4.530 g L^{-1})
DLN	13	18–19 Aug 2025	116.514720–116.710670	43.231267–43.376468	7,990–9,780 (7.990–9.780 g L^{-1})
DH	12	22–23 Aug 2025	112.639928–112.730132	40.558840–40.600557	7,990–8,960 (7.990–8.960 g L^{-1})

Note: Reported total-salt ranges are shown in both mg L^{-1} and g L^{-1}.

Table 2 Complete reporting of additive site-level linear models and J7 sensitivity analyses. The four primary salinity models included lake identity and within-lake-centered total salts; their J7-excluded sensitivity models used the same specification after recalculating the within-lake centering. The two cross-trophic models included lake identity and a within-lake-centered phytoplankton predictor. Full-data and cross-trophic models used n = 51 sites and residual df = 46; J7-excluded salinity models used n = 50 and residual df = 45

Analysis and response	Scale	Slope	HC3 95% CI	HC3 robust F	P	Model R^2	Diagnostics
Phytoplankton taxon richness	Full; per 1 g L^{-1}	0.739	−2.045 to 3.523	0.285	0.5957	0.702	SW P = 0.0024; BP P = 0.0003
Zooplankton taxon richness	Full; per 1 g L^{-1}	−0.962	−4.113 to 2.188	0.378	0.5416	0.493	SW P = 0.0598; BP P = 0.0015
Phytoplankton Shannon diversity	Full; per 1 g L^{-1}	0.142	−0.040 to 0.324	2.468	0.1231	0.403	SW P = 0.1875; BP P = 0.0667
Zooplankton Shannon diversity	Full; per 1 g L^{-1}	0.064	−0.072 to 0.199	0.902	0.3473	0.306	SW P = 0.7901; BP P = 0.5512
Cross-trophic density	$\log_{10}$	0.096	−0.216 to 0.408	0.383	0.5393	0.229	SW P = 0.8240; BP P = 0.0141
Cross-trophic richness	original	0.075	−0.181 to 0.332	0.348	0.5580	0.485	SW P = 0.0128; BP P = 0.0061
Phytoplankton taxon richness	J7 excluded; per 1 g L^{-1}	−0.563	−4.541 to 3.414	0.081	0.7768	0.701	SW P = 0.0070; BP P = 0.0003
Zooplankton taxon richness	J7 excluded; per 1 g L^{-1}	0.586	−0.526 to 1.699	1.126	0.2943	0.504	SW P = 0.0133; BP P = 0.0011
Phytoplankton Shannon diversity	J7 excluded; per 1 g L^{-1}	0.081	−0.437 to 0.598	0.099	0.7546	0.402	SW P = 0.2595; BP P = 0.0696
Zooplankton Shannon diversity	J7 excluded; per 1 g L^{-1}	0.100	−0.306 to 0.506	0.246	0.6225	0.299	SW P = 0.7912; BP P = 0.6637

Note: Slope is the focal unstandardized effect size. F and P use HC3 heteroscedasticity-consistent standard errors. SW = Shapiro–Wilk residual-normality diagnostic; BP = Breusch–Pagan heteroscedasticity diagnostic. Diagnostic P values below 0.05 indicate a departure; HC3 inference was used uniformly because departures occurred in several models.

Table 3 Descriptive multivariate location summaries and PERMDISP diagnostics for the four lake point clouds

Community	n	NMDS stress	Descriptive pseudo-F(3, 47)	R^2	PERMDISP F(3, 47)	P	Mean distance to median WLSH/JYH/DLN/DH
Phytoplankton	51	0.161	5.468	0.259	5.438	0.002	0.587 / 0.610 / 0.648 / 0.358
Zooplankton	51	0.112	7.775	0.332	9.186	0.001	0.388 / 0.456 / 0.188 / 0.201

Note: R^2 is the descriptive proportion of compositional variation associated with lake identity; PERMDISP tests heterogeneity of multivariate dispersion.

649 **Table 4** Pairwise DNCI estimates, method-specific intervals and balanced sample sizes

Community	Lake pair	Balanced n per lake	Median DNCI	Method-specific interval	Classification
Phytoplankton	DLN–DH	12	−6.660	−9.094 to −4.056	Dispersal-supported
Phytoplankton	JYH–DH	7	−2.934	−5.032 to −0.811	Dispersal-supported
Phytoplankton	JYH–DLN	7	−2.369	−4.652 to −0.268	Dispersal-supported
Phytoplankton	WLSH–DH	12	−3.880	−5.003 to −2.664	Dispersal-supported
Phytoplankton	WLSH–DLN	13	−3.072	−4.125 to −1.944	Dispersal-supported
Phytoplankton	WLSH–JYH	7	−2.413	−3.942 to −0.716	Dispersal-supported
Zooplankton	DLN–DH	12	−5.695	−7.566 to −3.789	Dispersal-supported
Zooplankton	JYH–DH	7	−2.302	−4.909 to 0.313	Uncertain
Zooplankton	JYH–DLN	7	−2.217	−5.146 to 0.642	Uncertain
Zooplankton	WLSH–DH	12	−3.274	−4.726 to −1.820	Dispersal-supported
Zooplankton	WLSH–DLN	12	−2.496	−3.962 to −1.041	Dispersal-supported
Zooplankton	WLSH–JYH	7	−1.668	−3.484 to 0.426	Uncertain

650

References

American Public Health Association (APHA), American Water Works Association (AWWA), Water Environment Federation (WEF) (2017) Standard methods for the examination of water and wastewater, 23rd edn. APHA Press, Washington, DC

Anderson MJ (2001) A new method for non-parametric multivariate analysis of variance. Austral Ecol 26:32–46. https://doi.org/10.1111/j.1442-9993.2001.01070.pp.x

Anderson MJ (2006) Distance-based tests for homogeneity of multivariate dispersions. Biometrics 62:245–253. https://doi.org/10.1111/j.1541-0420.2005.00440.x

Baselga A (2010) Partitioning the turnover and nestedness components of beta diversity. Glob Ecol Biogeogr 19:134–143. https://doi.org/10.1111/j.1466-8238.2009.00490.x

Bray JR, Curtis JT (1957) An ordination of the upland forest communities of southern Wisconsin. Ecol Monogr 27:325–349. https://doi.org/10.2307/1942268

Carvalho L, Poikane S, Lyche Solheim A et al (2013) Strength and uncertainty of phytoplankton metrics for assessing eutrophication impacts in lakes. Hydrobiologia 704:127–140. https://doi.org/10.1007/s10750-012-1344-1

Chase JM, Myers JA (2011) Disentangling the importance of ecological niches from stochastic processes across scales. Philos Trans R Soc B Biol Sci 366:2351–2363. https://doi.org/10.1098/rstb.2011.0063

Chen Q, Zhang J, Liu Y, Jiang H, Liu G, Yin X (2026) Nutrient-driven shifts in zooplankton structural-functional dynamics across different types of freshwater systems. Water Biol Secur 5:100449. https://doi.org/10.1016/j.watbs.2025.100449

Cunillera-Montcusí D, Beklioğlu M, Cañedo-Argüelles M et al (2022) Freshwater salinisation: a research agenda for a saltier world. Trends Ecol Evol 37:440–453. https://doi.org/10.1016/j.tree.2021.12.005

Deng M, Ma R, Loiselle SA et al (2024) Monitoring salinity in Inner Mongolian lakes based on Sentinel-2 images and machine learning. Remote Sens 16:3881. https://doi.org/10.3390/rs16203881

Foissner W, Berger H (1996) A user-friendly guide to the ciliates (Protozoa, Ciliophora) commonly used by hydrobiologists as bioindicators in rivers, lakes, and waste waters, with notes on their ecology. Freshw Biol 35:375–482. https://doi.org/10.1111/j.1365-2427.1996.tb01775.x

Gardolinski PCFC, Worsfold PJ, McKelvie ID (2004) Seawater induced release and transformation of organic and inorganic phosphorus from river sediments. Water Res 38:688–692. https://doi.org/10.1016/j.watres.2003.10.048

Geng Y, Lei X, Yu R et al (2024) Geographically driven shifts in land use influence phytoplankton community patterns in the Inner Mongolian Plateau lakes. J Plant Ecol 17:rtae058. https://doi.org/10.1093/jpe/rtae058

Gibert C, Escarguel G (2025) DNCImper: assembly process identification based on SIMPER analysis. R package version 0.0.1.7000. https://github.com/Corentin-Gibert-Paleontology/DNCImper. Accessed 28 September 2026

690 Gu P, Jia J, Qi D et al (2024) Response of phytoplankton composition to environmental
691 stressors under humidification in three alpine lakes on the Qinghai–Tibet Plateau, C
692 hina. Front Microbiol 15:1370334. https://doi.org/10.3389/fmicb.2024.1370334
693 Herbert ER, Boon P, Burgin AJ et al (2015) A global perspective on wetland salinization:
694 ecological consequences of a growing threat to freshwater wetlands. Ecosphere 6:2
695 06. https://doi.org/10.1890/ES14-00534.1
696 Hintz WD, Relyea RA (2019) A review of the species, community, and ecosystem impac
697 ts of road salt salinisation in fresh waters. Freshw Biol 64:1081–1097. https://doi.or
698 g/10.1111/fwb.13286
699 King L, Wienhues G, Misra P et al (2024) Anthropogenic eutrophication drives major fo
700 od web changes in Mwanza Gulf, Lake Victoria. Ecosystems 27:577–591. https://doi.
701 org/10.1007/s10021-024-00908-x
702 Kiørboe T (2011) How zooplankton feed: mechanisms, traits and trade-offs. Biol Rev 86:
703 311–339. https://doi.org/10.1111/j.1469-185X.2010.00148.x
704 Kruskal JB (1964) Nonmetric multidimensional scaling: a numerical method. Psychometri
705 ka 29:115–129. https://doi.org/10.1007/BF02289694
706 Li W, Wang L, Zhang Y, Wu L, Zeng H, Tuo Z (2021) Determining the groundwater ba
707 sin and surface watershed boundary of Dalinuoer Lake in the middle of Inner Mong
708 olian Plateau, China and its impacts on the ecological environment. China Geol 4:4
709 98–508. https://doi.org/10.31035/cg2021066
710 Lin Q, Xu L, Hou J, Liu Z, Jeppesen E, Han BP (2017) Responses of trophic structure a
711 nd zooplankton community to salinity and temperature in Tibetan lakes: implication
712 for the effect of climate warming. Water Res 124:618–629. https://doi.org/10.1016/j.
713 watres.2017.07.078
714 Liu C, Wu F, Jiang X et al (2022) Salinity is a key determinant for the microeukaryotic
715 community in lake ecosystems of the Inner Mongolia Plateau, China. Front Microbi
716 ol 13:841686. https://doi.org/10.3389/fmicb.2022.841686
717 Liu C, Wu F, Jiang X et al (2023) Climate change causes salinity to become determinant
718 in shaping the microeukaryotic spatial distribution among the lakes of the Inner M
719 ongolia–Xinjiang Plateau. Microbiol Spectr 11:e03178-22. https://doi.org/10.1128/spe
720 ctrum.03178-22
721 Long JS, Ervin LH (2000) Using heteroscedasticity consistent standard errors in the linea
722 r regression model. Am Stat 54:217–224. https://doi.org/10.1080/00031305.2000.104
723 74549
724 Ma J, Yin X, Liu G, Song J (2024) Intensification of human land use decreases taxonom
725 ic, functional, and phylogenetic diversity of macroinvertebrate community in Weihe
726 River Basin, China. Diversity 16:513. https://doi.org/10.3390/d16090513
727 Ministry of Ecology and Environment of China (2021) HJ 1216–2021 Water quality—det
728 ermination of phytoplankton—0.1 mL chamber—microscope counting method. Minis
729 try of Ecology and Environment of China, Beijing [in Chinese]
730 Ministry of Ecology and Environment of China (2023) HJ 1296–2023 Technical guidelin
731 es for water ecological monitoring—aquatic organism monitoring and evaluation of
732 lakes and reservoirs (on trial). Ministry of Ecology and Environment of China, Beiji
733 ng [in Chinese]

Mo Y, Peng F, Gao X et al (2021) Low shifts in salinity determined assembly processes and network stability of microeukaryotic plankton communities in a subtropical urban reservoir. Microbiome 9:128. https://doi.org/10.1186/s40168-021-01079-w

Muylaert K, Pérez-Martínez C, Sánchez-Castillo P, Lauridsen T, Vanderstukken M, Declerck SAJ, van der Gucht K, Conde-Porcuna JM, Jeppesen E, De Meester L, Vyverman W (2010) Influence of nutrients, submerged macrophytes and zooplankton grazing on phytoplankton biomass and diversity along a latitudinal gradient in Europe. Hydrobiologia 653:79–90. https://doi.org/10.1007/s10750-010-0345-1

Ogden CG, Hedley RH (1980) An atlas of freshwater testate amoebae. British Museum (Natural History), London

Oksanen J, Simpson GL, Blanchet FG et al (2025) vegan: community ecology package. R package version 2.7-2. https://doi.org/10.32614/CRAN.package.vegan

Olli K, Tamminen T, Ptacnik R (2023) Predictable shifts in diversity and ecosystem function in phytoplankton communities along coastal salinity continua. Limnol Oceanogr Lett 8:173–180. https://doi.org/10.1002/lol2.10242

Pedersen TL (2025) patchwork: the composer of plots. R package version 1.3.2. https://doi.org/10.32614/CRAN.package.patchwork

Pedersen TL, Shemanarev M (2025) ragg: graphic devices based on AGG. R package version 1.5.0. https://doi.org/10.32614/CRAN.package.ragg

R Core Team (2026) R: a language and environment for statistical computing. R Foundation for Statistical Computing, Vienna. https://www.R-project.org/

Soininen J, Heino J, Wang J (2018) A meta-analysis of nestedness and turnover components of beta diversity across organisms and ecosystems. Glob Ecol Biogeogr 27:96–109. https://doi.org/10.1111/geb.12660

Søndergaard M, Jeppesen E, Lauridsen TL et al (2007) Lake restoration: successes, failures and long-term effects. J Appl Ecol 44:1095–1105. https://doi.org/10.1111/j.1365-2664.2007.01363.x

Stegen JC, Lin X, Fredrickson JK et al (2013) Quantifying community assembly processes and identifying features that impose them. ISME J 7:2069–2079. https://doi.org/10.1038/ismej.2013.93

Stenger-Kovács C, Béres VB, Buczkó K et al (2023) Diatom community response to inland water salinization: a review. Hydrobiologia 850:4627–4663. https://doi.org/10.1007/s10750-023-05167-w

Sun X, Zhang H, Wang Z, Huang T, Huang H (2023) Phytoplankton community response to environmental factors along a salinity gradient in a seagoing river, Tianjin, China. Microorganisms 11:75. https://doi.org/10.3390/microorganisms11010075

Tang X, Xie G, Shao K, Tian W, Gao G, Qin B (2021) Aquatic bacterial diversity, community composition and assembly in the semi-arid Inner Mongolia Plateau: combined effects of salinity and nutrient levels. Microorganisms 9:208. https://doi.org/10.3390/microorganisms9020208

Tarafdar L, Kim JY, Srichandan S, Mohapatra M, Muduli PR, Kumar A, Mishra DR, Rastogi G (2021) Responses of phytoplankton community structure and association to variability in environmental drivers in a tropical coastal lagoon. Sci Total Environ 783:146873. https://doi.org/10.1016/j.scitotenv.2021.146873

778 Telesh IV, Khlebovich VV (2010) Principal processes within the estuarine salinity gradien
779 t: a review. Mar Pollut Bull 61:149–155. https://doi.org/10.1016/j.marpolbul.2010.02.
780 008
781 Tolonen KT, Karjalainen J, Hämäläinen H, Nyholm K, Rahkola-Sorsa M, Cai Y, Heino J
782 (2020) Do the ecological drivers of lake littoral communities match and lead to co
783 ngruence between organism groups? Aquat Ecol 54:839–854. https://doi.org/10.1007/
784 s10452-020-09781-x
785 van Diggelen JMH, Lamers LPM, van Dijk G et al (2014) New insights into phosphorus
786 mobilisation from sulphur-rich sediments: time-dependent effects of salinisation. PL
787 oS One 9:e111106. https://doi.org/10.1371/journal.pone.0111106
788 Vellend M (2010) Conceptual synthesis in community ecology. Q Rev Biol 85:183–206.
789 https://doi.org/10.1086/652373
790 Vilmi A, Gibert C, Escarguel G et al (2021) Dispersal–niche continuum index: a new qu
791 antitative metric for assessing the relative importance of dispersal versus niche proc
792 esses in community assembly. Ecography 44:370–379. https://doi.org/10.1111/ecog.05
793 356
794 Wan F, Zhang F, Zheng X, Xiao L (2022) Study on ecological water demand and ecologi
795 cal water supplement in Wuliangsuhai Lake. Water 14:1262. https://doi.org/10.3390/
796 w14081262
797 Wang S, Xu C, Zhang W, Chen H, Zhang B (2022) Human-induced water loss from clos
798 ed inland lakes: hydrological simulations in China's Daihai Lake. J Hydrol 607:127
799 552. https://doi.org/10.1016/j.jhydrol.2022.127552
800 Wickham H (2016) ggplot2: elegant graphics for data analysis. Springer, Cham. https://do
801 i.org/10.1007/978-3-319-24277-4
802 Williams WD (1999) Salinisation: a major threat to water resources in the arid and semi-
803 arid regions of the world. Lakes Reserv Res Manag 4:85–91. https://doi.org/10.1046
804 /j.1440-1770.1999.00089.x
805 Wurtsbaugh WA, Miller C, Null SE et al (2017) Decline of the world's saline lakes. Nat
806 Geosci 10:816–821. https://doi.org/10.1038/ngeo3052
807 Xie Y, Zhang Y, Lan H, Mao L, Zeng S, Chen Y (2018) Investigating long-term trends o
808 f climate change and their spatial variations caused by regional and local environme
809 nts through data mining. J Geogr Sci 28:802–818. https://doi.org/10.1007/s11442-01
810 8-1506-9
811 Zhang J, Liu Y, Chen Q, Yin X (2025) Biodiversity and functional redundancy of fish as
812 semblages in relation to nutrient enrichment: a case study in a boreal river of China.
813 Hydrobiologia 852:2993–3004. https://doi.org/10.1007/s10750-025-05811-7
814 Zhang M, Wang S, Gao G, Fu B, Ye Z, Shen Q (2019) Exploring responses of lake area
815 to river regulation and implications for lake restoration in arid regions. Ecol Eng 1
816 28:18–26. https://doi.org/10.1016/j.ecoleng.2018.12.031
817 Zhang Z, Huang X (1991) Research methods of freshwater plankton. Science Press, Beiji
818 ng [in Chinese]
819 Zheng B, Yin X (2023) Assembly mechanism of macroinvertebrate metacommunities and
820 ecological factors of multiple aspects of beta diversity in a boreal river basin, Chin
821 a. Front Ecol Evol 11:1131403. https://doi.org/10.3389/fevo.2023.1131403

822 Zhou J, Ning D (2017) Stochastic community assembly: does it matter in microbial ecolo
823 gy? Microbiol Mol Biol Rev 81:e00002-17. https://doi.org/10.1128/MMBR.00002-17
824 Zhu P, Ma M, Jin Y, Yin X, Zhu Z, Wang S, Shang S (2026) Nutrient enrichment modul
825 ates phytoplankton biodiversity–resource use efficiency relationships in temperate la
826 kes and reservoirs of Northern China. Hydrobiologia 853:1937–1950. https://doi.org/
827 10.1007/s10750-025-06042-6
828

Supplementary Files

This is a list of supplementary files associated with this preprint. Click to download.

- SupplementaryMaterial.docx
- SupplementaryTableS2.Taxonomicinventoryandoccurrencebylakeassociatedsamplingsystem.xlsx